

Zr–E π -Bonding in Complexes Derived from E–H Additions to $\text{Cp}_2\text{Zr}(\text{P}(\text{C}_6\text{H}_2\text{-2,4,6-}t\text{-Bu}_3))(\text{PMe}_3)$

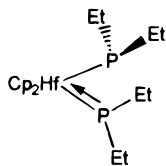
Tricia L. Breen and Douglas W. Stephan^{*,†}

Department of Chemistry and Biochemistry, University of Windsor,
Windsor, ON, Canada N9B 3P4

Received April 25, 1996[®]

Additions of PhEH ($\text{E} = \text{O}, \text{S}$), PhEH_2 ($\text{E} = \text{N}, \text{P}$), MesPH_2 , and Ph_2PH to $\text{Cp}_2\text{Zr}(\text{PR}^*)(\text{PMe}_3)$ (**2**) provide a facile route to complexes of the form $\text{Cp}_2\text{Zr}(\text{PHR}^*)(\text{ER})$ ($\text{R}^* = 2,4,6\text{-}t\text{-Bu-C}_6\text{H}_2$; $\text{ER} = \text{OPh}$ (**3**), SPh (**4**), NHPh (**5**), PPh (**6**), PMes (**7**), PPh_2 (**8**)). Variable-temperature NMR studies are consistent with facile metal-mediated inversion at phosphorus as well as rapid rotation about the Zr-E bonds at room temperature.

A feature common to early metal complexes of the form Cp_2MX_2 ($\text{M} = \text{Ti}, \text{Zr}, \text{Hf}$; $\text{X} = \text{OR}, \text{SR}, \text{NHR}, \text{PHR}$) is some degree of M-E π -bonding¹ arising from an interaction between lone pairs on E and the vacant $1a_1$ orbital of the Cp_2M fragment.² Perhaps one of the most striking examples of such π -bonding is illustrated by the structural study of $\text{Cp}_2\text{Hf}(\text{PETe}_2)_2$ by Baker et al.³ This species contains both pyramidal and planar phosphorus atoms consistent with the attainment of an 18-electron configuration at Hf via a Hf-P π -bond.



This localized bonding was also found in solution by variable-temperature NMR studies of the analogous $\text{Cp}_2\text{Hf}(\text{PCy}_2)_2$ complex. Although numerous studies have invoked arguments based on such π -interactions to account for both solution behavior and solid-state structures of early metal alkoxide, thiolate, amide, and phosphide complexes, related mixed-ligand systems have drawn little attention.¹ The absence of such studies is due in part to synthetic difficulties associated with the preparation of complexes of the form $\text{Cp}_2\text{M-X(Y)}$, where X and Y are potential π -donors. Recently, we reported the synthesis of $\text{Cp}_2\text{Zr}(\text{PR}^*)(\text{PMe}_3)$ (**2**) and demonstrated that the Zr-P double bond of **2** is highly reactive and readily undergoes cycloadditions, phosphinidene transfer reactions, and additions of group 14 halides.⁴ Herein we show that additions of PhEH ($\text{E} = \text{O}, \text{S}$), PhEH_2 ($\text{E} = \text{N}, \text{P}$), MesPH_2 , and Ph_2PH to **2** provide a facile route to complexes of the form $\text{Cp}_2\text{Zr}(\text{PHR}^*)(\text{ER})$ and $\text{Cp}_2\text{Zr}(\text{PHR}^*)(\text{EHR})$. Variable-temperature NMR studies of these species are reported, and the implications regarding Zr-P and Zr-E π -bonding are discussed.

Experimental Section

General Data. All preparations were done under an atmosphere of dry, O_2 -free N_2 by employing either Schlenk line techniques or a Vacuum Atmospheres inert-atmosphere glovebox. Solvents were reagent grade, distilled from the appropriate drying agents under N_2 and degassed by the freeze-thaw method at least three times prior to use. All organic reagents were purified by conventional methods. ^1H and $^{13}\text{C}\{^1\text{H}\}$ NMR spectra were recorded on a Bruker AC-300 operating at 300 and 75 MHz, respectively. ^{31}P and $^{31}\text{P}\{^1\text{H}\}$ NMR spectra were recorded on a Bruker AC-200 operating at 81 MHz. Trace amounts of protonated solvents were used as references, and chemical shifts are reported relative to SiMe_4 and 85% H_3PO_4 , respectively. Combustion analyses were performed by Galbraith Laboratories Inc., Knoxville, TN, or Schwarzkopf Laboratories, Woodside, NY. $\text{PH}_2(\text{C}_6\text{H}_2\text{-}t\text{-Bu}_3)$ was purchased from the Quantum Design Chemical Co. All other reagents were purchased from the Aldrich Chemical Co. $\text{Cp}_2\text{ZrMe}(\text{PHR}^*)$ (**1**) and $\text{Cp}_2\text{Zr}(\text{PR}^*)(\text{PMe}_3)$ (**2**) were prepared by literature methods.⁴ In all instances, R^* and Ar refer to the 2,4,6- $t\text{-Bu-C}_6\text{H}_2$ group.

^1H and ^{13}C NMR spectra of **1** acquired at 25 °C agreed with published data.⁴ ^1H NMR (–80 °C, $\text{CD}_3\text{C}_6\text{D}_5$): δ 7.74 (br s, 1H, Ar- H), 7.66 (br s, 1H, Ar- H), 5.57 (s, 5H, Cp), 5.30 (s, 5H, Cp), 1.86 (br s, 9H, $o\text{-}^t\text{Bu}$), 1.58 (br s, 9H, $o\text{-}^t\text{Bu}$), 1.33 (s, 9H, $p\text{-}^t\text{Bu}$), –0.07 (br s, 3H, Me). ^{31}P NMR (–80 °C, $\text{CD}_3\text{C}_6\text{D}_5$): δ 67.7 (d, $|J_{\text{P-H}}| = 261.5$ Hz).

Synthesis of $\text{Cp}_2\text{Zr}(\text{PHR}^*)(\text{OPh})$ (3**), $\text{Cp}_2\text{Zr}(\text{PHR}^*)(\text{NHPh})$ (**5**), and $\text{Cp}_2\text{Zr}(\text{PHR}^*)(\text{PPh}_2)$ (**8**).** These compounds were prepared in a similar manner; thus, only one representative preparation is given. To a benzene solution of **2** (114 mg, 0.4 mmol) was added phenol (18 mg, 0.4 mmol). The reaction mixture stood 1 h, after which time the solvent was removed in vacuo and the product dissolved in pentane. Yellow-brown crystals of **3** formed after this solution was allowed to stand for 12 h and were isolated by filtration.

3. Yield: 52%. ^1H NMR (25 °C, C_6D_6): δ 7.60 (d, $|^4J_{\text{P-H}}| = 1.8$ Hz, 2H, Ar- H), 7.20 (m, 2H, Ph- H), 6.85 (m, 1H, Ph- H), 6.61 (m, 2H, Ph- H), 5.66 (br s, 10, Cp), 5.29 (d, $|J_{\text{P-H}}| = 221.2$ Hz, 1H, P- H), 1.74 (br s, 18H, $o\text{-}^t\text{Bu}$), 1.35 (s, 9H, $p\text{-}^t\text{Bu}$). $^{13}\text{C}\{^1\text{H}\}$ NMR (25 °C, C_6D_6): δ 165.3 (s, quat), 146.0 (s, quat), 145.0 (d, $|J| = 36.8$ Hz, quat), 129.3 (s, arom. C- H), 121.0 (br s, arom C- H), 119.6 (s, arom C- H), 118.0 (s, arom C- H), 111.3 (s, Cp), 38.3 (br s, $o\text{-C}(\text{CH}_3)$), 34.6 (s, $p\text{-C}(\text{CH}_3)$), 33.1 (br s, $o\text{-C}(\text{CH}_3)$), 31.3 (s, $p\text{-C}(\text{CH}_3)$). ^{31}P NMR (25 °C, C_6D_6): δ –20.0 (d, $|J_{\text{P-H}}| = 220.6$ Hz). ^1H NMR (–70 °C, $\text{CD}_3\text{C}_6\text{D}_5$): δ 7.63 (br, 2H, Ar- H), 7.22–6.89 (m, 3H, Ph- H), 6.52 (m, 2H, Ph- H), 5.61 (s, 5H, Cp), 5.40 (s, 5H, Cp), 1.89 (s, 9H, $o\text{-}^t\text{Bu}$), 1.68 (s, 9H, $o\text{-}^t\text{Bu}$), 1.36 (s, 9H, $p\text{-}^t\text{Bu}$). ^{31}P NMR (–70 °C, $\text{CD}_3\text{C}_6\text{D}_5$): δ –22.4 (d, $|J_{\text{P-H}}| = 222.8$ Hz).

5. Yield: 78%. ^1H NMR (25 °C, C_6D_6): δ 7.60 (d, $|^4J_{\text{P-H}}| = 1.7$ Hz, 2H, Ar- H), 7.25–6.85 (m, 5H, Ph- H), 6.59 (s, 1H, N- H),

[†] E-mail: Stephan@UWindsor.ca.

[®] Abstract published in Advance ACS Abstracts, September 1, 1996.

(1) For leading references see: (a) Hey-Hawkins, E. *Chem. Rev.* **1994**, *94*, 1661. (b) Stephan, D. W. Nadasdi, T. T. *Coord. Chem. Rev.* **1996**, in press.

(2) Lauher, J.; Hoffmann, R. *J. Am. Chem. Soc.* **1976**, *98*, 1729.

(3) Baker, R. T.; Whitney, J. F.; Wreford, S. S. *Organometallics* **1983**, *2*, 1049.

(4) Breen, T. L.; Stephan, D. W. *J. Am. Chem. Soc.* **1995**, *117*, 11914.

5.51 (br s, 10H, Cp), 5.22 (d, $|J_{P-H}| = 223.2$ Hz, 1H, P-*H*), 1.68 (s, 18H, *o*-^tBu), 1.36 (s, 9H, *p*-^tBu). $^{13}\text{C}\{^1\text{H}\}$ NMR (25 °C, C_6D_6): δ 156.1 (s, quat), 155.8 (s, quat), 145.8 (s, quat), 144.6 (d, $|J| = 36.5$ Hz, quat), 120.9 (s, arom C-H), 120.6 (s, arom C-H), 120.5 (s, arom C-H), 119.4 (s, arom C-H), 109.7 (s, Cp), 38.2 (s, *o*-C(CH₃)₃), 34.6 (s, *p*-C(CH₃)₃), 32.7 (s, *o*-C(CH₃)₃), 31.3 (s, *p*-C(CH₃)₃). ^{31}P NMR (25 °C, C_6D_6): δ -11.1 (d, $|J_{P-H}| = 223.4$ Hz). ^1H NMR (-60 °C, $\text{CD}_3\text{C}_6\text{D}_5$): δ 7.72 (br s, 1H, Ar-*H*), 7.67 (br s, 1H, Ar-*H*), 7.37-6.75 (m, 5H, Ph-*H*), 6.60 (br s, 1H, N-*H*), 5.63 (s, 5H, Cp), 5.28 (d, $|J_{P-H}| = 223.0$ Hz, 1H, P-*H*), 5.22 (s, 5H, Cp), 1.79 (br s, 9H, *o*-^tBu), 1.70 (br s, 9H, *o*-^tBu), 1.41 (s, 9H, *p*-^tBu). ^{31}P NMR (-60 °C, $\text{CD}_3\text{C}_6\text{D}_5$): δ -13.6 (d, $|J_{P-H}| = 222.3$ Hz).

8. Yield: 85%. ^1H NMR (25 °C, C_6D_6): δ 7.64-6.98 (m, 12H, Ar-*H* and Ph-*H*), 6.67 (d, $|J_{P-H}| = 276.3$ Hz, 1H, P-*H*), 5.50 (s, 10H, Cp), 1.70 (br s, 18H, *o*-^tBu), 1.36 (s, 9H, *p*-^tBu). $^{13}\text{C}\{^1\text{H}\}$ NMR (25 °C, C_6D_6): δ 149.9 (s, quat), 148.8 (d, $|J| = 28.3$ Hz, quat), 135.1 (d, $|J| = 8.0$ Hz, quat), 134.0 (d, $|J| = 15.2$ Hz, arom C-H), 134.0 (d, $|J| = 16.9$ Hz, arom C-H), 124.9 (s, arom C-H), 121.7 (br s, arom C-H), 106.9 (s, Cp), 38.8 (s, *o*-C(CH₃)₃), 34.8 (s, *p*-C(CH₃)₃), 32.9 (s, *o*-C(CH₃)₃), 31.2 (s, *p*-C(CH₃)₃). ^{31}P NMR (25 °C, C_6D_6): δ 153.2 (dd, $|^2J_{P-P}| = 21.9$ Hz, $|J_{P-H}| = 278.9$ Hz), 17.4 (d, $|^2J_{P-P}| = 21.9$ Hz). ^1H NMR (-70 °C, $\text{CD}_3\text{C}_6\text{D}_5$): δ 7.75-7.00 (m, 12H, Ar-*H* and Ph-*H*), 5.54 (s, 5H, Cp), 5.40 (s, 5H, Cp), 2.00 (br s, 9H, *o*-^tBu), 1.47 (br s, 9H, *o*-^tBu), 1.32 (s, 9H, *p*-^tBu). ^{31}P NMR (-70 °C, $\text{CD}_3\text{C}_6\text{D}_5$): δ 164.6 (br d, $|J_{P-H}| = 292.4$ Hz), 5.0 (d, $|^2J_{P-P}| = 20.7$ Hz).

Generation of $\text{Cp}_2\text{Zr}(\text{PHR}^*)(\text{SPh})$ (4), $\text{Cp}_2\text{Zr}(\text{PHR}^*)(\text{PHPh})$ (6), and $\text{Cp}_2\text{Zr}(\text{PHR}^*)(\text{PHMes})$ (7). These compounds were generated in a similar manner; thus, only one representative preparation is given. To a benzene solution of **2** (114 mg, 0.4 mmol) was added thiophenol (20.4 μL , 0.4 mmol). The reaction mixture stood 10 min, after which time the solvent was removed in vacuo. The residue was characterized by NMR, although the unstable product degraded after 24 h in solution.

4. Yield: 76% (by ^1H NMR). ^1H NMR (25 °C, C_6D_6): δ 7.84-6.98 (m, 7H, Ph-*H* and Ar-*H*), 5.96 (d, $|J_{P-H}| = 259.3$ Hz, 1H, P-*H*), 5.56 (s, 10, Cp), 1.70 (br s, 18H, *o*-^tBu), 1.32 (s, 9H, *p*-^tBu). $^{13}\text{C}\{^1\text{H}\}$ NMR (25 °C, C_6D_6): δ 154.2 (d, $|J| = 7.5$ Hz, quat), 148.1 (s, quat), 147.4 (s, quat), 139.5 (d, $|J| = 12.1$ Hz, quat), 133.8 (s, arom C-H), 124.3 (s, arom C-H), 122.0 (s, arom C-H), 121.4 (br s, arom C-H), 109.2 (s, Cp), 38.6 (br s, *o*-C(CH₃)₃), 34.7 (s, *p*-C(CH₃)₃), 32.9 (br s, *o*-C(CH₃)₃), 31.3 (s, *p*-C(CH₃)₃). ^{31}P NMR (25 °C, C_6D_6): δ 64.4 (d, $|J_{P-H}| = 259.3$ Hz). ^1H NMR (-50 °C, $\text{CD}_3\text{C}_6\text{D}_5$): δ 7.93-7.07 (m, 7H, Ph-*H* and Ar-*H*), 5.54 (s, 5H, Cp), 5.45 (s, 5H, Cp), 1.99 (br s, 9H, *o*-^tBu), 1.53 (br s, 9H, *o*-^tBu), 1.32 (s, 9H, *p*-^tBu). ^{31}P NMR (-70 °C, $\text{CD}_3\text{C}_6\text{D}_5$): δ 63.9 (d, $|J_{P-H}| = 259.3$ Hz).

6. Yield: 92% (by ^1H NMR). ^1H NMR (25 °C, C_6D_6): δ 7.67-6.98 (m, 7H, Ar-*H* and Ph-*H*), 6.60 (d, $|J_{P-H}| = 291.4$ Hz, 1H, P-*H*), 5.43 (s, 10, Cp), 3.36 (dd, $|J_{P-H}| = 188.0$ Hz, $|^3J_{P-H}| = 15.4$ Hz, 1H, P-*H*), 1.65 (br s, 18H, *o*-^tBu), 1.28 (s, 9H, *p*-^tBu). $^{13}\text{C}\{^1\text{H}\}$ NMR (25 °C, C_6D_6): δ 150.3 (s, quat), 149.9 (s, quat), 133.2 (d, $|J| = 12.7$ Hz, arom C-H), 128.4 (s, arom C-H), 123.7 (s, arom C-H), 121.7 (s, arom C-H), 107.1 (s, Cp), 38.7 (br s, *o*-C(CH₃)₃), 34.8 (s, *p*-C(CH₃)₃), 32.8 (br s, *o*-C(CH₃)₃), 31.2 (s, *p*-C(CH₃)₃). ^{31}P NMR (25 °C, C_6D_6): δ 151.9 (d, $|J_{P-H}| = 291.2$ Hz), -43.6 (d, $|J_{P-H}| = 187.7$ Hz). ^1H NMR (-80 °C, $\text{CD}_3\text{C}_6\text{D}_5$): δ 7.73-6.96 (m, 7H, Ar-*H* and Ph-*H*), 6.38 (d, $|J_{P-H}| = 291.6$ Hz, 1H, P-*H*), 5.38 (s, 5H, Cp), 5.23 (s, 5H, Cp), 3.20 (br dd, $|J_{P-H}| = 180$ Hz, $|^3J_{P-H}| = 16$ Hz, 1H, P-*H*), 1.77 (br s, 9H, *o*-^tBu), 1.45 (br s, 9H, *o*-^tBu), 1.31 (s, 9H, *p*-^tBu). ^{31}P NMR (-80 °C, $\text{CD}_3\text{C}_6\text{D}_5$): δ 155.1 (d, $|J_{P-H}| = 294.9$ Hz), -46.6 (d, $|J_{P-H}| = 183.1$ Hz).

7. Yield: 94% (by ^1H NMR). ^1H NMR (25 °C, C_6D_6): δ 7.63 (s, 2H, Ar-*H*), 7.01 (s, 2H, Ar-*H*), 6.38 (d, $|J_{P-H}| = 283.0$ Hz, 1H, P-*H*), 5.36 (s, 10H, Cp), 3.53 (dd, $|J_{P-H}| = 205.7$ Hz, $|^3J_{P-H}| = 12.8$ Hz, 1H, P-*H*), 2.51 (s, 6H, *o*-Me), 2.30 (s, 3H, *p*-Me), 1.66 (br s, 18H, *o*-^tBu), 1.35 (s, 9H, *p*-^tBu). $^{13}\text{C}\{^1\text{H}\}$ NMR (25 °C, C_6D_6): δ 149.4 (s, quat), 144.7 (s, quat), 138.4 (d, $|J| = 9.9$

Table 1. Crystallographic Data

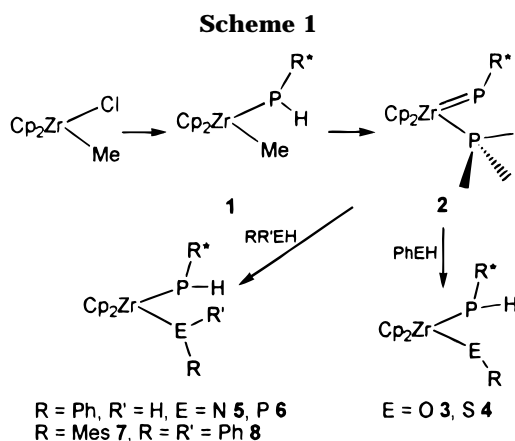
formula	$\text{C}_{34}\text{H}_{46}\text{PNZr}$
fw	590.94
cryst color, form	blocks
cryst size	$0.30 \times 0.25 \times 0.25$
<i>a</i> (Å)	9.627(4)
<i>b</i> (Å)	21.063(7)
<i>c</i> (Å)	16.227(4)
β (deg)	106.30(3)
cryst syst	monoclinic
space group	$P2_1/n$
<i>V</i> (Å ³)	3158(2)
<i>D</i> _{calcd} (g cm ⁻³)	1.24
<i>Z</i>	4
abs coeff, μ , cm ⁻¹	4.20
radiation (λ (Å))	Mo K α (0.710 69)
temp (°C)	24
scan speed, deg/min	16 ($\theta/2\theta$) (1-3 scans)
scan range (deg)	1.0 above K α_1 , 1.0 below K α_2
bkgd/scan ratio	0.5
data collcd	5747
2θ range (deg)	4.5-50
index range	$\pm h, k, l$
data $F_o^2 > 3\sigma(F_o^2)$	2075
variables	284
transm factors	0.818-0.996
<i>R</i> (%) ^a	7.3
<i>R</i> _w (%) ^a	5.5
largest Δ/σ	0
goodness of fit	2.76

$$^a R = \sum ||F_o| - |F_c|| / \sum |F_o|; R_w = [\sum (|F_o| - |F_c|)^2 / \sum |F_o|^2]^{0.5}.$$

Hz, quat), 133.4 (s, quat), 121.6 (br s, arom C-H), 119.7 (s, arom C-H), 107.2 (s, Cp), 38.6 (br s, *o*-C(CH₃)₃), 34.8 (s, *p*-C(CH₃)₃), 32.8 (br s, *o*-C(CH₃)₃), 31.2 (s, *p*-C(CH₃)₃), 24.8 (d, $|^3J_{P-P}| = 9.4$ Hz, *o*-Me), 20.9 (s, *p*-Me). ^{31}P NMR (25 °C, C_6D_6): δ 130.6 (ddd, $|J_{P-H}| = 282.5$ Hz, $|^2J_{P-P}| = 36.6$ Hz, $|^3J_{P-H}| = 14.3$ Hz), -60.4 (d, $|J_{P-H}| = 206.1$ Hz, $|^2J_{P-P}| = 36.6$ Hz). ^1H NMR (-70 °C, $\text{CD}_3\text{C}_6\text{D}_5$): δ 7.78 (br s, 2H, Ar-*H*), 7.69 (br s, 2H, Ar-*H*), 5.96 (d, $|J_{P-H}| = 286.1$ Hz, 1H, P-*H*), 5.29 (s, 5H, Cp), 5.23 (s, 5H, Cp), 3.42 (br dd, $|J_{P-H}| = 204.2$ Hz, $|^3J_{P-H}| = 15$ Hz, 1H, P-*H*), 2.55 (br s, 6H, *o*-Me), 2.40 (s, 3H, *p*-Me), 1.92 (br s, 9H, *o*-^tBu), 1.54 (br s, 9H, *o*-^tBu), 1.34 (s, 9H, *p*-^tBu). ^{31}P NMR (-70 °C, $\text{CD}_3\text{C}_6\text{D}_5$): δ 142.2 (br d, $|J_{P-H}| = 286.8$ Hz), -69.7 (dd, $|J_{P-H}| = 204.1$ Hz, $|^2J_{P-P}| = 24.4$ Hz).

X-ray Data Collection and Reduction. X-ray-quality crystals of **5** were obtained directly from the preparation as described above. The crystal was manipulated and mounted in capillaries in a glovebox, thus maintaining a dry, O₂-free environment for each crystal. Diffraction experiments were performed on a Rigaku AFC6 diffractometer equipped with graphite-monochromatized Mo K α radiation. The initial orientation matrix was obtained from 20 machine-centered reflections selected by an automated peak search routine. These data were used to determine the crystal system. Automated Laue system check routines around each axis were consistent with the crystal system. Ultimately, 25 reflections ($20^\circ < 2\theta < 25^\circ$) were used to obtain the final lattice parameters and the orientation matrix. Crystal data are summarized in Table 1. The observed extinctions were consistent with the space groups. The data were collected in three shells ($4.5^\circ < 2\theta < 50.0^\circ$), and three standard reflections were recorded every 197 reflections. Fixed scan rates were employed. Up to 4 repetitive scans of each reflection at the respective scan rates were averaged to ensure meaningful statistics. The number of scans of each reflection was determined by the intensity. The intensities of the standards showed no statistically significant change over the duration of data collection. The data were processed using the TEXSAN crystal solution package operating on a SGI Challenger mainframe with remote X-terminals. The reflections with $F_o^2 > 3\sigma(F_o^2)$ were used in the refinements.

Structure Solution and Refinement. Non-hydrogen atomic scattering factors were taken from the literature



tabulations.^{5,6} The Zr atom position was determined using direct methods. The remaining non-hydrogen atoms were located from successive difference Fourier map calculations. The refinement was carried out by using full-matrix least-squares techniques on F , minimizing the function $w(|F_o| - |F_c|)^2$, where the weight w is defined as $4F_o^2/2\sigma(F_o^2)$ and F_o and F_c are the observed and calculated structure factor amplitudes. In the final cycle of refinement, all the non-hydrogen atoms were assigned anisotropic temperature factors. An empirical absorption correction was applied to the data sets based on ψ -scan data. C-H hydrogen atom positions were calculated and allowed to ride on the carbon to which they are bonded assuming a C-H bond length of 0.95 Å. The N-H and P-H hydrogen atoms were located in a difference Fourier map and their contributions included but not refined in subsequent least-squares calculations. Hydrogen atom temperature factors were fixed at 1.10 times the isotropic temperature factor of the carbon atom to which they are bonded. The hydrogen atom contributions were calculated but not refined. The final values of R , R_w , and the maximum Δ/σ on any of the parameters in the final cycle of refinement are given in Table 1. The locations of the largest peak in the final difference Fourier map calculation as well as the magnitude of the residual electron density were of no chemical significance. Positional parameters, hydrogen atom parameters, thermal parameters, and bond distances and angles have been deposited as Supporting Information.

Results and Discussion

Synthesis. We have previously reported that elimination of methane from $\text{Cp}_2\text{ZrMe}(\text{PHR}^*)$ (**1**) affords, upon trapping with PMe_3 , the terminal phosphinidene complex $\text{Cp}_2\text{Zr}(\text{PR}^*)(\text{PMe}_3)$ (**2**) (Scheme 1).⁴ Protic reagents such as phenol, aniline, thiophenol, and primary or secondary phosphines react rapidly with **2** to yield a series of compounds of the form $\text{Cp}_2\text{Zr}(\text{PHR}^*)(\text{ER})$ ($\text{ER} = \text{OPh}$ (**3**), SPh (**4**), NHPh (**5**), PHPh (**6**), PHMes (**7**), PPh_2 (**8**)). In each case, ^{31}P NMR spectra were consistent with E-H addition across the $\text{Zr}=\text{P}$ double bond, as evidenced by the P-H coupling in the resulting supermesitylphosphide ligands as well as the P-P coupling in **7** and **8**. ^1H NMR data also supported the formulations above. Although these compounds could be generated and characterized spectroscopically, they proved difficult to isolate due to their extreme solubility in organic solvents. In addition, the thermal

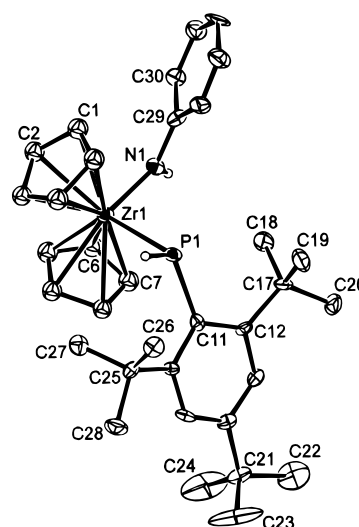


Figure 1. ORTEP drawing of **5** with 30% thermal ellipsoids shown. Distances (Å) and angles (deg): Zr-P 2.707(4), Zr-N 2.09(1), P-C 1.86(1), N-C 1.38(1); P-Zr-N 99.0(3).

instability of compounds **4** and **6-8** resulted in either disproportionation or elimination of organophosphine over a 24 h period at 25 °C. The latter degradation pathway is consistent with established reactivity of zirconocene bis(organophosphides).⁷

The formulation of **5** was verified by a single-crystal diffraction study (Figure 1). As expected, the geometry about the zirconium atom of **5** is pseudo-tetrahedral, with two η^5 -cyclopentadienyl ligands, a supermesitylphosphide, and a phenylamido ligand completing the coordination sphere. The location of both the amido and phosphido hydrogen atoms confirmed a pseudo-trigonal planar geometry at nitrogen, and a pseudo-tetrahedral geometry at phosphorus. The Zr-P distance (2.707(4) Å) in **5** is considerably longer than the Zr-P bonds in $\text{Cp}_2\text{Zr}(\text{PHR}^*)\text{Cl}$ (2.558(7) Å),⁸ $(\text{MeCp})_2\text{Zr}(\text{PH}(2,4,6\text{-}i\text{-Pr}_3\text{C}_6\text{H}_2)\text{Cl})$ (2.6381(8) Å),⁹ and $\text{Cp}_2\text{Zr}(\text{PHR}^*)_2$ (2.681(5), 2.682(5) Å).¹⁰ Moreover, the Zr-N bond length of 2.09(1) Å is shorter than the Zr-N bonds in $\text{Cp}_2\text{Zr}(\text{NC}_4\text{H}_4)_2$ (2.171(2), 2.167(2) Å) and $\text{Cp}_2\text{Zr}(\text{NCO})_2$ (2.117(7) Å).¹¹ The P-Zr-N angle of 99.0(3)° in **5** compares with the Cl-Zr-P angles of 97.1(2) and 93.55(2)° in $\text{Cp}_2\text{Zr}(\text{PHR}^*)\text{Cl}$ ⁸ and $(\text{MeCp})_2\text{Zr}(\text{PH}(2,4,6\text{-}i\text{-Pr}_3\text{C}_6\text{H}_2)\text{Cl})$ ⁹, respectively. The larger angle in **5** may be credited to the greater steric demands of the substituents on the two ancillary ligands. These data are consistent with a formal single Zr-P bond and strong π -character in the Zr-N bond of **5**.

Temperature-Dependent NMR Data. NMR spectra for compounds **1** and **3-8** were recorded over a temperature range 30 to -80 °C. Marked temperature dependences were observed in each case. In each of these compounds, the resonances attributable to the *ortho-tert*-butyl groups of the supermesityl substituents are broad at 25 °C and split into two resonances upon

(5) (a) Cromer, D. T.; Mann, J. B. *Acta Crystallogr., Sect. A: Cryst. Phys., Theor. Gen. Crystallogr.* 1968, A24, 324. (b) Cromer, D. T.; Mann, J. B. *Acta Crystallogr., Sect. A: Cryst. Phys., Theor. Gen. Crystallogr.* 1968, A24, 390.

(6) Cromer, D. T.; Waber, J. T. *International Tables for X-ray Crystallography*; Knoch Press: Birmingham, England, 1974.

(7) (a) Hou, Z.; Stephan, D. W. *J. Am. Chem. Soc.* 1992, 114, 10088. (b) Hou, Z.; Breen, T. L.; Stephan, D. W. *Organometallics* 1993, 12, 3158.

(8) Hey, E.; Lappert, M. F.; Atwood, J. L.; Bott, S. G. *Polyhedron* 1988, 7, 2083.

(9) Hey-Hawkins, E.; Kurz, S. Z. *Naturforsch.* 1995, 50b, 239.

(10) Hey-Hawkins, E.; Kurz, S. *J. Organomet.* 1994, 479, 125.

(11) Vann Bynum, R.; Hunter, W. E.; Rogers, R. D.; Atwood, J. L. *Inorg. Chem.* 1980, 19, 2368.

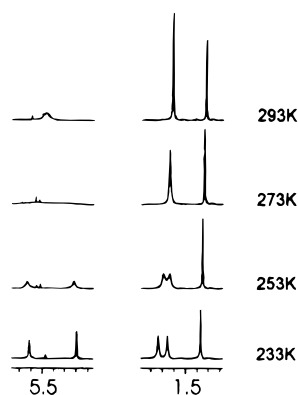


Figure 2. Variable-temperature ^1H NMR spectrum for **5**.

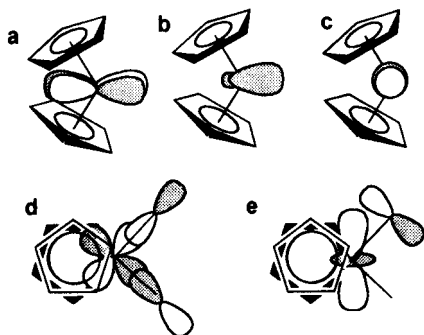
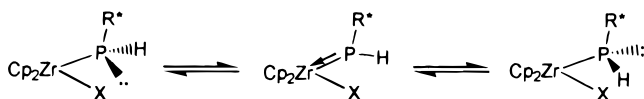


Figure 3. Schematic depiction of the (a) $2a_1$, (b) b_2 , and (c) $1a_1$ orbitals of the Cp_2M fragment, (d) σ -interaction of the b_2 orbital of the Cp_2M fragment with the ligand σ orbitals, and (e) π -interaction of the ligand p-orbital with the $1a_1$ orbital.

Scheme 2



cooling. This temperature dependence results from sterically inhibited rotation about the P–C bond, a feature common to systems with sterically demanding substituents.¹⁰ In addition, a second dynamic process may be distinguished for these compounds. As the temperature is lowered, the broad resonance due to the cyclopentadienyl rings splits and eventually sharpens into two lines (Figure 2). ΔG_c^\ddagger values pertaining to this process were determined to be 11.8, 13.1, 13.1, 13.4, 12.5, 12.4, and 12.4, and 12.4 ± 1 kcal mol^{−1} for compounds **1** and **3–8**.

Inequivalent cyclopentadienyl groups in these complexes arise as a result of the incorporation of a PHR* ligand which provides a chiral phosphorus center and, consequently, diastereotopic cyclopentadienyl ligands. The dynamic process which results in a single cyclopentadienyl ring environment at room temperature must therefore involve facile inversion at P in addition to rapid rotation about the Zr–E bond (Scheme 2). Related metal-mediated epimerization of transition metal phosphide complexes,^{12–17} as well as rotational barriers about early metal π -bonds to amide,^{18,19} alkoxide, and thiolate ligands,²⁰ have been studied both

experimentally and via computational studies. The barriers for the dynamic processes observed herein are in accord with those previously reported for transition metal mediated P inversion and are significantly lower than the barrier to inversion for organophosphines.^{21,22} Zr–P π -bonding accounts for this reduction in the energy barrier and is accomplished by alignment of the P p-orbital with the LUMO or $1a_1$ orbital of the Cp_2M fragment.² This orbital is oriented in the plane which lies between the cyclopentadienyl ligands, hence in the plane of the ancillary donor atoms (Figure 3). The aforementioned Zr–P π -bonding is maximized by a planar geometry at P, which has been observed in the solid-state structure of $\text{Cp}_2\text{Hf}(\text{PEt}_2)_2$.³ In the diphosphide complexes **6–8**, the disparate nature of the ^{31}P NMR resonances is consistent with pyramidal and planar geometries at the phosphorus atoms. The presence of this dative Zr–P bond reflects the Lewis acidity of the Zr center, which achieves a formal 18-electron count. For compound **8**, the P–H coupling of 292 Hz associated with the low-field resonance indicates that it is the supermesitylphosphide ligand that participates in π -bonding. NOE experiments designed to probe this question for **6** and **7** were inconclusive. Compound **5** exhibits a relatively high-field ^{31}P NMR resonance consistent with a pyramidal geometry at phosphorus, while Zr–N π -bonding is confirmed by the crystallographic data (*vide supra*). Similarly, the ^{31}P NMR data for compounds **1**, **3**, and **4** imply pyramidal P geometries. Although unconfirmed, Zr–O and Zr–S π -bonding analogous to that seen in **5** is anticipated in **3** and **4**, respectively. Structural studies of complexes of the form $\text{Cp}_2\text{Zr}(\text{ER})_2$ (E = O, S)²⁰ support this notion. It should be noted, however, that other related studies of early metal chalcogenide species by the groups of Parkin and Rothwell conclude that structural data does not support M–E π bonding.²³ Furthermore, the upfield chemical shift of the cyclopentadienyl rings for **3** and **4** are consistent with a formal 18-electron configuration at the metal center. The comparatively low barrier to inversion observed for **1** is ascribed to strong σ -donation by the methyl group to Zr, while the rotational barriers about the Zr–P bonds in **6–8** are consistent with the greater steric demands of the ancillary phosphide substituents. In comparison, the steric inhibition in Cp_2 -

(14) (a) Crisp, G. T.; Salem, G.; Wild, S. B. *Organometallics* **1989**, *8*, 2360. (b) Crisp, G. T.; Salem, G.; Stephens, F. S.; Wild, S. B. *J. Chem. Soc., Chem. Commun.* **1987**, 600.

(15) (a) Zwick, B. D.; Dewey, M. A.; Knight, D. A.; Buhro, W. E.; Arif, A. M.; Gladysz, J. A. *Organometallics* **1992**, *11*, 2673. (b) Buhro, W. E.; Zwick, B. D.; Georgiou, S.; Hutchinson, J. P.; Gladysz, J. A. *J. Am. Chem. Soc.* **1988**, *110*, 2427.

(16) Rogers, J. R.; Wagner, T. P. S.; Marynick, D. S. *Inorg. Chem.* **1994**, *33*, 3104.

(17) Jorg, K.; Malisch, W.; Reich, W.; Meyer, A.; Schubert, U. *Angew. Chem., Int. Ed. Engl.* **1986**, *25*, 92.

(18) (a) Hillhouse, G. L.; Bulls, A. R.; Santarsiero, B. D.; Bercaw, J. E. *Organometallics* **1988**, *7*, 1309. (b) Hillhouse, G. L.; Bercaw, J. E. *Organometallics* **1982**, *1*, 1025.

(19) (a) Chrisholm, M. H.; Cotton, F. A.; Extine, Stults, B. R. *J. Am. Chem. Soc.* **1976**, *98*, 4477. (b) Chisholm, M. H.; Cotton, F. A.; Frenz, B. A.; Reichert, W. W.; Shive, L. W.; Stults, B. R. *J. Am. Chem. Soc.* **1976**, *98*, 4469.

(20) Stephan, D. W.; Nadasdi, T. T. *Coord. Chem. Rev.* **1996**, *147*, 147.

(21) Macdonell, G. D.; Berlin, K. D.; Baker, J. R.; Ealick, S. E.; van der Helm, D.; Marsi, K. L. *J. Am. Chem. Soc.* **1978**, *100*, 4535.

(22) Schmidbaur, H.; Schier, A.; Lautenschlager, S.; Reide, J.; Muller, G. *Organometallics* **1984**, *3*, 1906.

(23) For a leading reference, see: (a) Howard, W. A.; Parkin, G. J. *Am. Chem. Soc.* **1994**, *116*, 606. (b) Profflet, R. D.; Fanwick, P. E.; Rothwell, I. P. *Angew. Chem., Int. Ed. Engl.* **1990**, *29*, 664.

(12) Roddick, D. M.; Santarsiero, B. D.; Bercaw, J. E. *J. Am. Chem. Soc.* **1985**, *107*, 4670.

(13) Bohra, R.; Hitchcock, P. B.; Lappert, M. F.; Leung, W.-P. *J. Chem. Soc., Chem. Commun.* **1989**, 728.

Hf(PCy₂)₂ and Cp*₂HfH(NHR)¹⁸ is substantially reduced, and the energies required to average the cyclopentadienyl rings are diminished to 6 and 10 kcal mol⁻¹, respectively.³

In summary, the reactivity of the Zr–P double bond of **2** affords the facile synthesis of complexes of the form Cp₂Zr(PHR*)(ER) and Cp₂Zr(PHR*)(EHR). Data presented herein illustrate that Zr–E π -interactions are generally weak and yet provide avenues for both metal-mediated pyramidal inversion at P and quenching of the Lewis acidity of electron deficient Zr centers. In addition, the strengths of such Zr–E π -bonds are dependent

on the nature of both the substituents and the other ancillary ligands in the complex.

Acknowledgment. Support from the NSERC of Canada is acknowledged. T.L.B. is grateful for the award of an NSERC postgraduate scholarship.

Supporting Information Available: Tables of positional parameters, hydrogen atom parameters, thermal parameters, and bond distances and angles (10 pages). Ordering information is given on any current masthead page.

OM960314O